

## Peptide functionalized superparamagnetic iron oxide nanoparticles as MRI contrast agents†

Selim Sulek,<sup>a</sup> Busra Mammadov,<sup>a</sup> Davut I. Mahcicek,<sup>b</sup> Huseyin Sozeri,<sup>c</sup> Ergin Atalar,<sup>bd</sup> Ayse B. Tekinay<sup>a</sup> and Mustafa O. Guler<sup>\*a</sup>

Received 2nd April 2011, Accepted 2nd August 2011

DOI: 10.1039/c1jm11387a

Magnetic resonance imaging (MRI) attracts great attention in cellular and molecular imaging due to its non-invasive and multidimensional tomographic capabilities. Development of new contrast agents is necessary to enhance the MRI signal in tissues of interest. Superparamagnetic iron oxide nanoparticles (SPIONs) are used as contrast agents for signal enhancement as they have revealed extraordinary magnetic properties at the nanometre size and their toxicity level is very low compared to other commercial contrast agents. In this study, we developed a new method to functionalize the surface of SPIONs. Peptide amphiphile molecules are used to coat SPIONs non-covalently to provide water solubility and to enhance biocompatibility. Superparamagnetic properties of the peptide-SPION complexes and their ability as contrast agents are demonstrated. *In vitro* cell culture experiments reveal that the peptide-SPION complexes are biocompatible and are localized around the cells due to their peptide coating.

## Introduction

Magnetic resonance imaging (MRI) is one of the most powerful non-invasive techniques for disease diagnosis. Due to its capability for providing high spatial resolution non-invasively and revealing three-dimensional anatomic details without any damage, it attracts intense interest in clinical studies and became one of the most powerful candidates for imaging techniques.<sup>1</sup> MRI can measure the water content of the tissue and excited nuclear spins of water molecules in different tissues create distinct signal intensities that enable detection of abnormal tissues.<sup>2</sup> MRI uses radiofrequency in a magnetic field as source of radiation which has no harmful effects on the body and

measures the relaxivity ( $r_1$  or  $r_2$ ) of the water protons in the tissue at a given magnetic field.<sup>3</sup> In spite of these excellent features, development of new contrast agents (CAs) is desired to enhance the precision of MRI. CAs mainly shorten the  $T_1$  or  $T_2$  relaxation times of protons located in the proximity.<sup>4,5</sup> Positive contrast agents reduce the relaxation time  $T_1$  which results in brighter contrast whereas negative contrast agents reduce the relaxation time  $T_2$  which results in darker contrast. There are numerous types of contrast agents on the market and gadolinium ( $Gd^{3+}$ ) based CAs are the most widely used in MRI. The most important drawback of the  $Gd^{3+}$  based CAs is their high toxicity.<sup>4</sup> Superparamagnetic iron oxide nanoparticles (SPIONs) are good alternatives as CAs for MRI because of their low level of toxicity, superparamagnetic properties and biocompatibility.<sup>6</sup>

Important parameters for SPIONs to be used as contrast agents are their magnetic properties, surface coating properties and molecular targeting potentials.<sup>7</sup> The magnetic properties of the SPIONs are controlled by their crystal structure, size and constituents.<sup>7,8</sup> Thermal decomposition enables the synthesis of monodisperse and crystalline SPIONs.<sup>9</sup> However, SPIONs produced by thermal decomposition generally have hydrophobic molecules on their surface. Several methods were developed to make these nanoparticles water soluble in order to enable their use in biological applications. Dextran and PEG polymers were previously used to solubilize SPIONs in water.<sup>5</sup> Dextran is a branched polysaccharide consisting of glucose subunits and was used for surface coating of SPIONs because of its biocompatibility and high blood circulation time due to its neutral charge.<sup>10</sup> PEG is a neutral linear polymer and can be prepared with a variety of terminal functional groups. Their neutral nature helps SPIONs to escape from phagocytes providing a longer blood circulation time. Although PEG and dextran increase blood circulation time of SPIONs, they lack bioactivity. Previously, SPIONs were also functionalized with folic acid for targeting purposes.<sup>11</sup> Although folic acid offers better specificity and selectivity than PEG or dextran, it is still not sufficient for accurate diagnosis since folic acid receptors are not sufficient for targeting. Researchers have focused on using proteins and peptides for targeted imaging and therapy for surface functionalization of the SPIONs. In conventional methods, peptides are conjugated to SPIONs covalently, however, peptide adsorption on nanoparticles is very complex.<sup>12</sup> In addition, protein and peptide adsorption on nanoparticles is irreversible in covalent functionalization and needs protecting groups to bind to proteins or peptides selectively.<sup>13</sup>

<sup>a</sup>UNAM-Institute of Materials Science and Nanotechnology, Bilkent University, Ankara, Turkey 06800. E-mail: moguler@unam.bilkent.edu.tr

<sup>b</sup>National Magnetic Resonance Research Center (UMRAM), Bilkent University, Ankara, Turkey 06800

<sup>c</sup>The Scientific and Technical Research Council of Turkey (TÜBİTAK), National Metrology Institute (UME), Gebze, Kocaeli, Turkey 41470

<sup>d</sup>Department of Electrical and Electronics Engineering, Bilkent University, Ankara, Turkey 06800

† Electronic supplementary information (ESI) available: The LC-MS results of the PA molecules and additional nanoparticle characterizations. See DOI: 10.1039/c1jm11387a

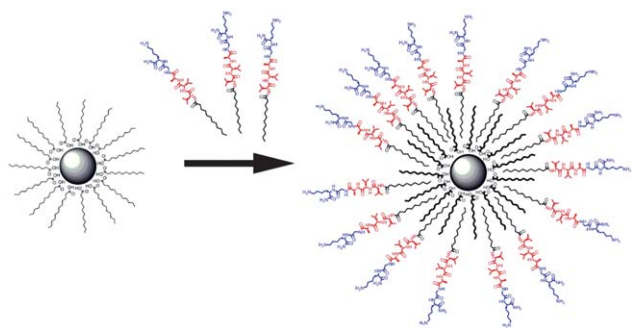


**Fig. 1** Non-covalent functionalization of SPIONs with peptide amphiphile molecules.

Herein, we demonstrate a new method to synthesize peptide functionalized SPION CAs (Fig. 1). We exploited amphiphilic peptide molecules as surfactants for the functionalization of SPIONs. The hydrophobic segment of the peptide amphiphiles and SPIONs interact non-covalently in aqueous conditions. Since the coating process depends on hydrophobic interactions, peptide adsorption on the nanoparticle surface is easier compared to covalent conjugation approaches. Hydrophobic interactions prevent changes in crystallinity of the nanoparticles and allow non-covalent functionalization to provide solubility in water. This technique provides opportunities for incorporation of bioactive groups without any further functionalization process.

## Experimental section

### Materials

Dibenzyl ether was purchased from Merck, lauryl amine was purchased from Sigma-Aldrich, iron 2,4-pentadionate ( $\text{Fe}(\text{acac})_3$ ) and lauric acid were purchased from Alfa Aesar. 1,2-Hexadecanediol was purchased from Sigma-Aldrich. 9-Fluorenylmethoxycarbonyl (Fmoc) and *tert*-butoxycarbonyl (Boc) protected amino acids, [4- $\alpha$ -(2',4'-dimethoxyphenyl)Fmoc-aminomethyl]phenoxy]acetamidonorleucyl-MBHA resin (Rink amide MBHA resin), Fmoc-Asp(OtBu)-Wang resin and 2-(1*H*-benzotriazol-1-yl)-1,1,3,3-tetramethyluronium hexafluorophosphate (HBTU) were purchased from NovaBiochem and ABCR. The other chemicals were purchased from Fisher, Merck, Alfa Aesar or Aldrich and used as provided.

### Peptide amphiphile (PA) synthesis

Lauryl-VVAGK peptide (**PA1**) was constructed on MBHA Rink amide resin and lauryl-VVAAD peptide (**PA2**) was constructed on Fmoc-Asp-(OtBu)-OH preloaded Wang resin. Amino acid couplings were performed with 2 equivalents of Fmoc protected amino acid, 1.95 equivalents of HBTU and 3 equivalents of *N,N*-diisopropylethylamine (DIEA) in DMF for 2 h. Fmoc deprotections were performed with 20% piperidine/dimethylformamide (DMF) solution for 20 min. Cleavage of the peptides from the resin was carried out with a mixture of trifluoroacetic acid (TFA) : triisopropylsilane (TIS) : water in the ratio of 95 : 2.5 : 2.5 for 2 h. Excess TFA was removed by rotary evaporation. The remaining viscous peptide solution was treated with ice-cold diethyl ether and the resulting white pellet was freeze-dried. The peptide amphiphiles were identified and analyzed by reverse phase HPLC on an Agilent 6530 accurate-Mass Q-TOF

LC/MS equipped with an Agilent 1200 HPLC. An Agilent Zorbax Extend-C18  $2.1 \times 50$  mm column for basic conditions and a Zorbax SB-C8  $4.6 \text{ mm} \times 100$  mm column for acidic conditions were used to analyze peptides. For **PA1**, the mobile phase was water/acetonitrile gradient with 0.1% volume of formic acid. For **PA2**, the mobile phase was water/acetonitrile gradient with 0.1%  $\text{NH}_4\text{OH}$ . Chemical representations of the peptides are demonstrated in Fig. S1.† Preparative HPLC (Agilent 1200) was used for purification of the peptides. **PA1** was purified by using a Zorbax prepHT 300CB-C8 column with a water–acetonitrile (0.1% TFA) gradient. **PA2** purification was performed on a Zorbax Extend C-18 prep-HT with a water–acetonitrile (0.1%  $\text{NH}_4\text{OH}$ ) gradient. The HPLC and mass spectrum of **PA1** are shown in Fig. S2–S3 and HPLC and mass spectrum of **PA2** are presented in Fig. S4–S5.†

### Superparamagnetic iron oxide nanoparticle synthesis

Magnetite ( $\text{Fe}_3\text{O}_4$ ) nanoparticles were synthesized as previously reported with slight modifications in the synthesis protocol.<sup>9</sup> 2 mmol  $\text{Fe}(\text{acac})_3$ , 10 mmol 1,2-hexadecanediol, 6 mmol lauric acid and 6 mmol lauryl amine were dissolved in 20 ml of benzyl ether. The solution was deoxygenated with nitrogen gas and magnetically stirred while heating up to  $200^\circ\text{C}$  for 2 h. Then, the solution was refluxed at  $270^\circ\text{C}$  for 1 h. It was cooled to room temperature and 50 ml ethanol was added. The solution was centrifuged at 8000 rpm for 10 min. Precipitated nanoparticles were collected and more ethanol was added and centrifuged at 8000 rpm for 10 min. The nanoparticles were dissolved in hexanes in the presence of 1 mmol lauric acid and sonicated for 10 min. Then the solution was centrifuged at 8000 rpm for 10 min. The magnetic properties of the samples were determined at room temperature using the vibrating sample magnetometer (LDJ, Electronics Inc., Model 9600) with a maximum field of up to 15 kOe.

### Non-covalent functionalization of superparamagnetic iron oxide nanoparticles

30 mg of **PA1** was dissolved in 3 ml distilled water and the pH of the solution was adjusted to pH 2. Then  $10 \text{ mg ml}^{-1}$  SPION stock solution in hexane was prepared. Peptide amphiphiles and SPIONs were mixed with a weight ratio of 1 : 7.  $35 \text{ mg}/3.5 \text{ ml}$  of peptide amphiphile solution was then sonicated for 5 min and  $5 \text{ mg}/0.35 \text{ ml}$  of SPION solution was poured into the PA solution. The mixture was shaken for a couple of seconds and sonicated for 1 min. This step was repeated for 10 min and sonication was performed for 1 h at  $60^\circ\text{C}$ . The solution was heated to  $60^\circ\text{C}$  and then sonicated for 1 h more at  $60^\circ\text{C}$ . The same process was repeated for **PA2** at pH 11. Then, the solution was filtered through a  $1 \mu\text{m}$  PTFE filter and 1 ml dichloromethane was poured into the solution which was then shaken for a couple of seconds and centrifuged at 8000 rpm for 2 min. This step was repeated 3 times. Solutions were dialyzed with 500–1000 Da cellulose dialysis membrane. A representative drawing of noncovalent functionalization is shown in Fig. 1.

### Dynamic light scattering

Hydrodynamic size and polydispersity index of the particles were measured by dynamic light scattering (DLS). A Malvern Nanosizer/Zetasizer<sup>®</sup> nano-ZS ZEN 3600 (Malvern Instruments, USA) instrument was used for DLS analysis. Hydrophobic particles were diluted with hexane and measurements were performed in a quartz cuvette.

The hydrophilic particles were diluted with water and measurements were performed in a polystyrene cuvette.

### X-Ray diffraction (XRD)

A Panalytical X'PERT Pro MRD was used to perform XRD diffraction pattern analysis under Cu-K $\alpha$  radiation. A solution of lauric acid coated magnetic nanoparticles was deposited on a glass substrate and the solvent was evaporated off.

### FT-IR

A Bruker VERTEX 70 with a Hyperion Scanning Microscope was used for the FT-IR analysis. Hydrophobic nanoparticle solution was dropped onto sodium chloride glass and air-dried. Transmittance characterization was done between 370 and 4000 cm<sup>-1</sup>.

### Cell viability

Mouse embryonic fibroblast cells (NIH 3T3) were used to analyze the effect of SPIONs on cell viability. NIH 3T3 cells were cultured in DMEM supplemented with 10% calf serum. Cells were seeded in 96 well plates (5000 cells/well) and varying concentrations of SPIONs (500  $\mu\text{g ml}^{-1}$ , 200  $\mu\text{g ml}^{-1}$ , 100  $\mu\text{g ml}^{-1}$ , 50  $\mu\text{g ml}^{-1}$ ) were added 24 h later at pH 7. Live/dead assay from Invitrogen was used to detect live cells by Calcein AM (2  $\mu\text{M}$ ) and dead cells by ethidium homodimer 1 (2  $\mu\text{M}$ ) 48 h after the addition of SPIONs. Fluorescence measurements were taken by a M5 microplate reader (Molecular Devices). Peptides that are not coupled with iron oxide nanoparticles were used as control at the same concentrations.

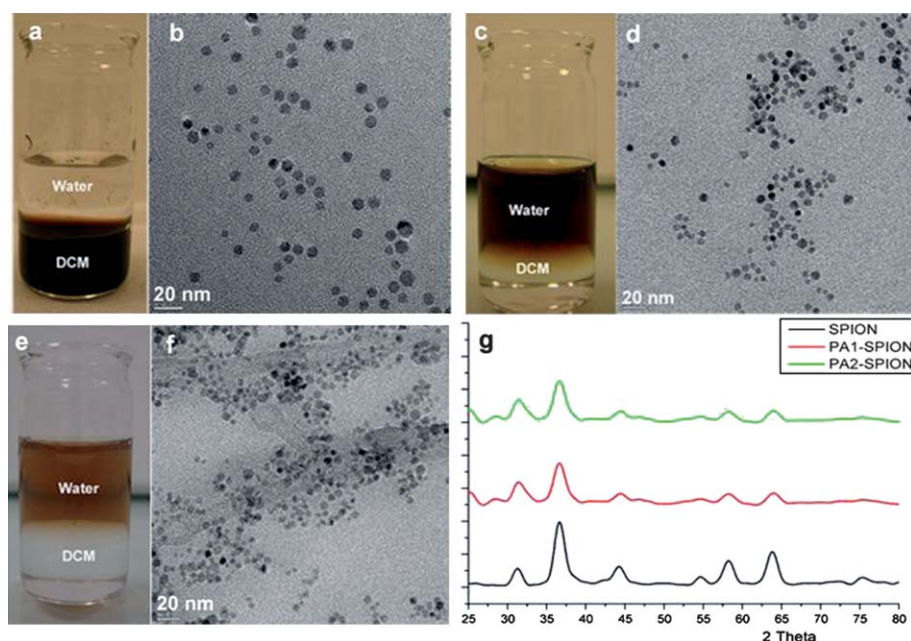
### Prussian blue staining

To detect cell internalization and localization of SPIONs, cells were stained with Prussian Blue (PB). NIH 3T3 cells were seeded in 96 well

plates 3000 cells/well) and 24 h after seeding cells, SPIONs were added (500  $\mu\text{g ml}^{-1}$ ) at pH 7. 24 h after addition of SPIONs, PB staining was performed. After washing wells with PBS several times, cells were fixed with 4% paraformaldehyde. A fresh mixture of 2% HCl + 2% K<sub>4</sub>Fe(CN)<sub>6</sub> (1 : 1) was then added to the cells and incubated at room temperature for 30 min. After washing with PBS several times, images were taken under an inverted microscope (Zeiss). The iron content was quantitatively determined by the colorimetric PB assay and measured by a Spectramax M5 (Molecular Devices). Samples were prepared by mixing 200  $\mu\text{l}$  of PA1-SPION, PA2-SPION or their diluted solution with 200  $\mu\text{l}$  of 6 N HCl for 1 h at 60 °C. The iron content of samples was calculated by comparing the absorbance to that of a range of standard concentrations of equal volume.

### Magnetic resonance imaging

MRI measurements of the peptide coated SPIONs were performed on a Siemens 3T TIMTrio Scanner (Siemens Medical Solutions, Erlangen, Germany). Peptide coated SPIONs were dispersed in water and diluted to various concentrations (0.0375, 0.075, 0.15, 0.2, 0.5 mM) and the pH of the solutions was adjusted to 7. A 5 ml glass sample holder was placed in the iso-center of the magnet. Spin-echo pulse sequences with multiple spin echoes of various echo times were utilized to obtain pixel-by-pixel  $T_1$  and  $T_2$  maps of each sample.  $T_1$  and  $T_2$  relaxation times were measured from large regions of interest and results were inverted to obtain the  $R_1$  and  $R_2$  relaxation rates in s<sup>-1</sup>. MR imaging capabilities of the SPIONs were examined at 3 T with the following parameters: point resolution: 0.11–0.11 cm, section thickness: 2.3 mm, TE: 11, 13, 15, 18, 20, 30, 50, 100, 200, 500 ms, TR: 3000 ms; another set of experiments were set up with the following parameters: TR: 100, 200, 500, 1000, 2000, 5000 ms, TE: 11 ms, number of acquisitions: 3. As  $T_2$  and  $T_1$  weighted images were obtained with various echo times,  $T_2$  and  $T_1$  values were calculated

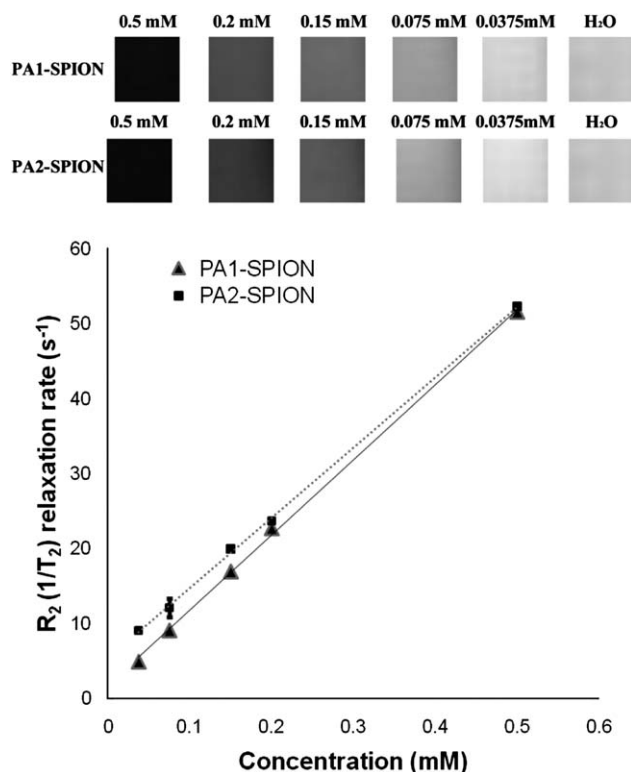


**Fig. 2** a) Dichloromethane (DCM)–water phase image of lauric acid coated SPIONs. b) TEM image of lauric acid coated SPION. c) DCM–water phase image of PA1-SPION complex. d) TEM image of PA1-SPION complex. e) DCM–water phase image of PA2-SPION. f) TEM image of PA2-SPION. g) XRD pattern of lauric acid coated SPION, PA1-SPION and PA2-SPION.



**Table 1** Physicochemical properties of peptide–SPION complexes

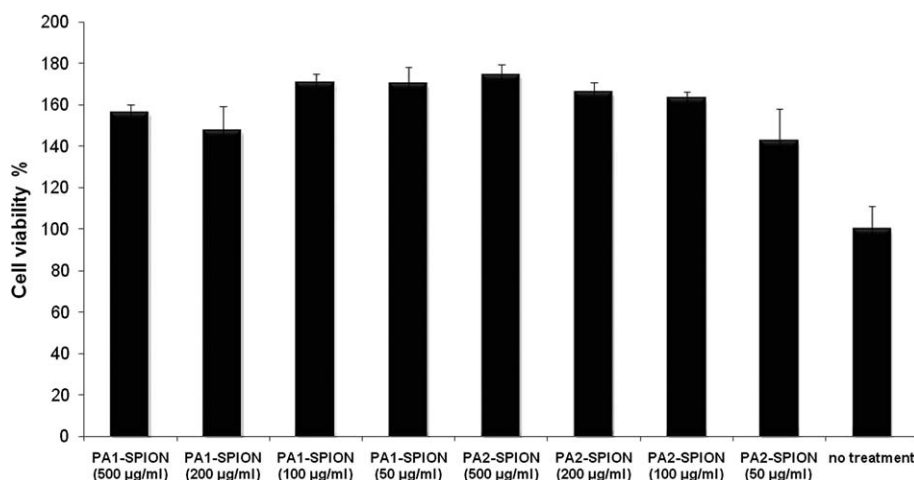
SPION coating	Size by TEM (nm)	Size by DLS (nm)	Transversal relaxivity ( $r_2$ ) ( $s^{-1} \text{ mM}^{-1}$ )	$r_2/r_1$	Saturation magnetization ( $M_s$ ) ( $\text{emu g}^{-1}$ )
Lauric acid	7 nm	8–10 nm	—	—	53
PA1	24 nm	24–32 nm	100.4	111.55	8
PA2	30 nm	26–38 nm	93.7	55.1	5

**Fig. 3** Contrast images of the peptide–SPION complexes measured at  $TR = 3000$  ms and  $TE = 50$  ms (top). Relaxation rates ( $1/T_2$ ,  $s^{-1}$ ) of PA1-SPION and PA2-SPION as a function of iron concentration in water in a magnetic field of 3 T at room temperature (bottom).

using the curve fitting toolbox of Matlab. The  $r_1$  and  $r_2$  values were calculated based on  $1/T_2$  and  $1/T_1$  versus iron concentration determined with Prussian blue colorimetric assay.

## Results and discussion

SPIONs were synthesized by the thermal decomposition method which produces uniform nanoparticles.<sup>9</sup> We were able to synthesize monodisperse nanoparticles with diameters of 6–7 nm without aggregation (Fig. 2b). Lauric acid was used as a surfactant on the SPIONs and the end products were stable in organic solvents (Fig. 2a). Numerous efforts have been previously reported aiming to coat these particles with hydrophilic molecules (silanization,<sup>14</sup> polymers,<sup>15</sup> protein absorption,<sup>16</sup> *etc.*). Recently, amphiphilic polymers were used to transfer the SPIONs into aqueous solutions.<sup>15</sup> Polymers require a covalent attachment process to provide bioactivity and/or biocompatibility. In this study, we developed a new method to solubilize SPIONs in water by using peptide amphiphile (PA) molecules. The hydrophobic part of the PAs is composed of lauric acid which intercalates hydrophobically with lauric acid chains covering the SPIONs (Fig. 1). The hydrophilic peptide segment of the PA molecule is exposed at the exterior part of the SPIONs and provides stability and bioactivity in aqueous conditions.<sup>17</sup> The PAs can be modified by various peptide sequences for targeting desired cell types and/or molecules. The optimum ratio for the synthesis of the peptide–SPION complex was found to be 7 mg PA to 1 mg SPION and the optimum volume for the mixture is 10 ml PA solution in water to 1 ml of SPIONs in hexane. Excess amount of PA was used with the optimum dilution to prevent aggregation of SPIONs. The excess amount of SPIONs was removed *via* filtration through a 0.20  $\mu\text{m}$

**Fig. 4** Cell viability assay, 48 h after addition of SPIONs on NIH 3T3 cells revealed that treatment with peptide coated SPIONs enhanced cell viability with respect to uncoated SPIONs and no treatment.

filter and centrifugation. Afterwards, the solutions were dialyzed with 500–1000 Dalton cellulose membrane bags to remove excess PAs. The hysteresis loop of the SPIONs was measured by VSM to study superparamagnetic behavior at room temperature. As shown in Fig. S7†, the SPIONs have zero coercivity field and do not reach saturation at high fields indicating that these nanoparticles are superparamagnetic. Fig. S7 also shows the magnetization curves of synthesized SPIONs before and after functionalization processes. The saturation magnetization ( $M_s$ ) of a lauric acid stabilized SPION sample was found to be  $56 \text{ emu g}^{-1}$ . After functionalization process,  $M_s$  of **PA1**-SPION decreased to  $5 \text{ emu g}^{-1}$  and  $M_s$  of **PA2**-SPION decreased to  $8 \text{ emu g}^{-1}$ . The decrease in  $M_s$  value was caused by the peptide coating.<sup>18</sup>

TEM characterization of SPIONs revealed a narrow size distribution even with the PA coating (about 25–40 nm in diameter) (Table 1, Fig. 2 and Fig. S6). XRD pattern shown in Fig. 2g demonstrates that SPIONs were synthesized in magnetite form without any changes in their crystallinity. In Fig. 2a, c and e, the effects of surface coating on the solubility of the SPIONs are demonstrated. The lauric acid coated SPIONs were stable in dichloromethane solution. After surface coating, the SPIONs were successfully transferred into aqueous solution. The FT-IR spectrum in Fig. S9† revealed amine and amide peaks due to the presence of peptide on the SPIONs.

Hydrophobic encapsulation of SPIONs by PAs changes the size of the particles. The TEM images of the SPIONs reveal that the nanoparticle size is around 8–10 nm in diameter (Table 1 and Fig. 2). Peptide coated nanoparticles were imaged by TEM directly (Fig. 2) and by staining with uranyl acetate and phosphotungstic acid to observe the effect of the peptide segment. The sizes of the peptide coated nanoparticles were increased significantly. In addition, the hydrodynamic size of the peptide coated SPIONs was also measured by the DLS technique. The increase in size upon encapsulation was also observed in DLS (Table 1). The size increase can be explained by the nonspecific aggregation of the PA molecules. The amount of PA molecules may be more than the amount needed to solubilize the nanoparticles because of the aggregation tendency of the PA molecules.

SPIONs are negative contrast agents and reduce the  $T_2$  relaxation time of water protons resulting in darker signals. Relaxation rates  $R_1$  and  $R_2$ , which are the reciprocals of the relaxation times, reveal the relaxivity values  $r_1$  and  $r_2$  of SPIONs depending on the total metal concentration. These values determine the effectiveness of the SPIONs as a contrast agent. The relaxivity values are investigated under 3 T magnetic field and the  $r_1$  and  $r_2$  relaxivity values of **PA1**-SPION are  $0.9 \text{ mM}^{-1} \text{ s}^{-1}$  and  $100.4 \text{ mM}^{-1} \text{ s}^{-1}$ , whereas  $r_1$  and  $r_2$  values of **PA2**-SPION are  $1.8 \text{ mM}^{-1} \text{ s}^{-1}$  and  $93.7 \text{ mM}^{-1} \text{ s}^{-1}$  respectively in water as shown in Table 1 and Fig. 3. It is known that the  $r_2/r_1$  ratio is an important parameter to determine the  $T_2$  contrast agent efficiency. The  $r_2/r_1$  ratio for **PA1**-SPION is 111.55 and it is 52.1 for **PA2**-SPION. The  $r_2$  relaxivity values observed here are close to those of commercial SPIONs and their particle size is much smaller, whereas the  $r_2/r_1$  ratio is much greater than the commercial ones.<sup>19–22</sup>

The biocompatibility of the peptide coated nanoparticles was tested by culturing NIH 3T3 cells. The number of viable cells incubated with peptide–SPION complex was increased up to 170% compared to cells not treated with peptide–SPION (Fig. 4). These results revealed that peptide–SPION complexes are highly biocompatible. The increase in cell viability is due to peptide coatings which

provide mechanical support for cells, similar to the natural extracellular matrix. In order to test this, the cell viability test was repeated with cells treated with PA molecules without magnetic nanoparticles. Results indicated that PA molecules caused the increase in cell viability (Fig. S8†). We also carried out Prussian blue staining to observe where these nanoparticles were located in the cells. Staining was carried out 24 h after addition of peptide–SPION complex to the cells. Positively charged **PA1**-SPIONs were observed to be located on the cell membrane or matrix whereas negatively charged **PA2**-SPION complexes could not bind to cells and were removed from the medium in the PBS washing step (Fig. 5). The positively charged molecules are attracted to the cell membrane because of the negative charge of the cell surface.

By using peptide amphiphile molecules, we developed water soluble and biocompatible SPIONs as MRI contrast agents. Peptide

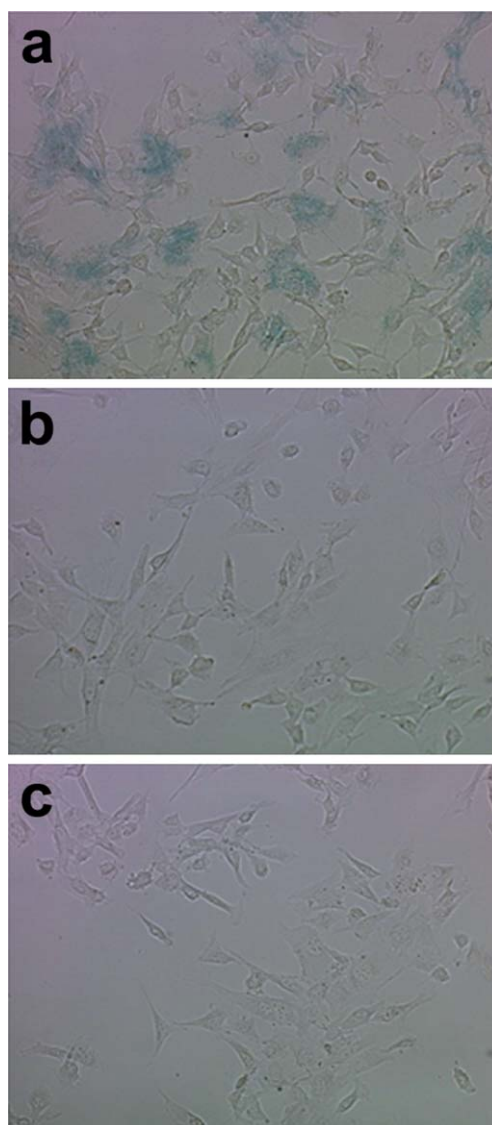


**Fig. 5** NIH 3T3 cells stained by Prussian blue reaction after 24 h treatment. a) **PA1**-SPION, b) **PA2**-SPION, c) negative control. Positively charged SPIONs are bound to the cell surface more than negatively charged or uncoated SPIONs because of the negatively charged nature of the cell surface.

amphiphile molecules provided stability in aqueous solutions, bio-functionality through their peptide sequence and enhanced physico-chemical properties for SPIONs. Their ability to be used as MRI contrast agents is demonstrated in Table 1. Peptide synthesis enables control over peptide sequences<sup>23</sup> for specific and selective localization of nanoparticles to target cells. By using homing peptide sequences,<sup>24</sup> it is possible to target organs such as brain,<sup>25</sup> kidney,<sup>25</sup> heart,<sup>26</sup> breast<sup>24</sup> and several tumor tissues.<sup>27,28</sup> Thus, by using non-covalent functionalization of SPIONs with appropriate peptide sequences, cellular or molecular targeting is possible without any further coupling process.

## Conclusion

This study presents a novel method for coating SPIONs based on intercalation of PA molecules with SPIONs by hydrophobic interactions. The hydrophobic encapsulation of SPIONs by PA molecules provided solubility in water and enabled us to overcome problems associated with surfactant exchange for SPION coating. *In vitro* cell culture experiments revealed that the peptide-SPION complex is a biocompatible system. Their use as MRI contrast agents is also demonstrated. MR active system shown here can be selectively functionalized by using various peptide molecules for targeting specific tissues. Potential applications of these materials for tissue engineering, biological separation and biosensor applications are under investigation.

## Acknowledgements

This research was supported by the Scientific and Technological Research Council of Turkey (TÜBİTAK) 110S386. We would like to thank Z. Erdogan for help in LC-MS, M. Guler for help in TEM, E. Kahveci for help in XRD and Prof. M. Toprak for helpful discussions. M.O.G. acknowledges support from the Turkish Academy of Sciences Distinguished Young Scientist Award (TUBA GEBİP).

## References

- 1 V. Chandra, J. Park, Y. Chun, J. W. Lee, I.-C. Hwang and K. S. Kim, *ACS Nano*, 2010, **4**, 3979–3986.

- 2 M. A. Brown, R. C. Semelka, *MRI: Basic Principles and Applications*, Wiley: Hoboken, New York, 2005.
- 3 C. S. S. R. Kumar, *Nanomaterials for Cancer Diagnosis*, Wiley-VCH, Weinheim, 2006.
- 4 P. Caravan, J. J. Ellison, T. J. McMurphy and R. B. Lauffer, *Chem. Rev.*, 1999, **99**, 2293–2352.
- 5 R. Qiao, C. Yang and M. Gao, *J. Mater. Chem.*, 2009, **19**, 6274–6293.
- 6 J. W. M. Bulte and D. L. Kraitchman, *NMR Biomed.*, 2004, **17**, 484–499.
- 7 Y.-w. Jun, J.-H. Lee and J. Cheon, *Angew. Chem., Int. Ed.*, 2008, **47**, 5122–5135.
- 8 S. Tong, S. Hou, Z. Zheng, J. Zhou and G. Bao, *Nano Lett.*, 2010, 4607–4613.
- 9 S. Sun, H. Zeng, D. B. Robinson, S. Raoux, P. M. Rice, S. X. Wang and G. Li, *J. Am. Chem. Soc.*, 2003, **126**, 273–279.
- 10 T. Shen, R. Weissleder, M. Papisov, A. Bogdanov and T. J. Brady, *Magn. Reson. Med.*, 1993, **29**, 599–604.
- 11 S. Mohapatra, *et al.*, *Nanotechnology*, 2007, **18**, 385102.
- 12 D. Aili and M. M. Stevens, *Chem. Soc. Rev.*, 2010, **39**, 3358–3370.
- 13 I. M. Rio-Echevarria, R. Tavano, V. Causin, E. Papini, F. Mancin and A. Moretto, *J. Am. Chem. Soc.*, 2010, **133**, 8–11.
- 14 J. Kim, H. S. Kim, N. Lee, T. Kim, H. Kim, T. Yu, I. C. Song, W. K. Moon and T. Hyeon, *Angew. Chem., Int. Ed.*, 2008, **47**, 8438–8441.
- 15 M. Moros, B. Pelaz, P. Lopez-Larrubia, M. L. Garcia-Martin, V. Grazu and J. M. d. l. Fuente, *Nanoscale*, 2010, **2**, 1746–1755.
- 16 C. H. Yu, A. Al-Saadi, S.-J. Shih, L. Qiu, K. Y. Tam and S. C. Tsang, *J. Phys. Chem. C*, 2008, **113**, 537–543.
- 17 S. Toksöz and M. O. Guler, *Nano Today*, 2009, **4**, 458–469.
- 18 P. Tartaj and C. J. Serna, *J. Am. Chem. Soc.*, 2003, **125**, 15754–15755.
- 19 R. Weissleder, D. D. Stark, B. L. Engelstad, B. R. Bacon, C. C. Compton, D. L. White, P. Jacobs and J. Lewis, *Am. J. Roentgenol.*, 1989, **152**, 167–173.
- 20 P. Reimer, E. J. Rummeny, H. E. Daldrop, T. Balzer, B. Tombach, T. Berns and P. E. Peters, *Radiology*, 1995, **195**, 489–496.
- 21 C. W. Jung and P. Jacobs, *Magn. Reson. Imaging*, 1995, **13**, 661–674.
- 22 L. Wang, K. G. Neoh, E. T. Kang, B. Shuter and S.-C. Wang, *Adv. Funct. Mater.*, 2009, **19**, 2615–2622.
- 23 P. D. W. W. C. Chan, *Fmoc Solid Phase Peptide Synthesis A Practical Approach*, Oxford University Press Inc., New York, 2004.
- 24 M. Essler and E. Ruoslahti, *Proc. Natl. Acad. Sci. U. S. A.*, 2002, **99**, 2252–2257.
- 25 R. Pasqualini and E. Ruoslahti, *Nature*, 1996, **380**, 364–366.
- 26 L. Zhang, J. A. Hoffman and E. Ruoslahti, *Circulation*, 2005, **112**, 1601–1611.
- 27 W. Arap, R. Pasqualini and E. Ruoslahti, *Science*, 1998, **279**, 377–380.
- 28 R. Pasqualini, E. Koivunen, R. Kain, J. Lahdenranta, M. Sakamoto, A. Stryhn, R. A. Ashmun, L. H. Shapiro, W. Arap and E. Ruoslahti, *Cancer Res.*, 2000, **60**, 722–727.